Electronic Supplementary Information (ESI)

Effect of π-Conjugated Bridges of TPD-based Medium Bandgap Conjugated Copolymers for Efficient Tandem Organic Photovoltaic Cells

Ji-Hoon Kim,[a] Jong Baek Park,[a] Fei Xu,[a] Dongwook Kim,[b] Jeonghun Kwak,[c]

Andrew C. Grimsdale,[d] Do-Hoon Hwang[a]*

[a]*Department of Chemistry, and Chemistry Institute for Functional Materials, Pusan National University, Busan 609-735, Republic of Korea*

[b]*Department of Chemistry, Kyonggi University, San 94-6, Iui-dong, Yeongtong-gu,*

Suwonsi, Gyeonggi 443-760, Republic of Korea.

[c]*Department of Electronic Engineering, Dong-A University, Busan 604-714,*

Republic of Korea

[d]*School of Materials Science and Engineering, Nanyang Technological University, 50 Nanyang Avenue, Singapore 639798*

Table of the Contents

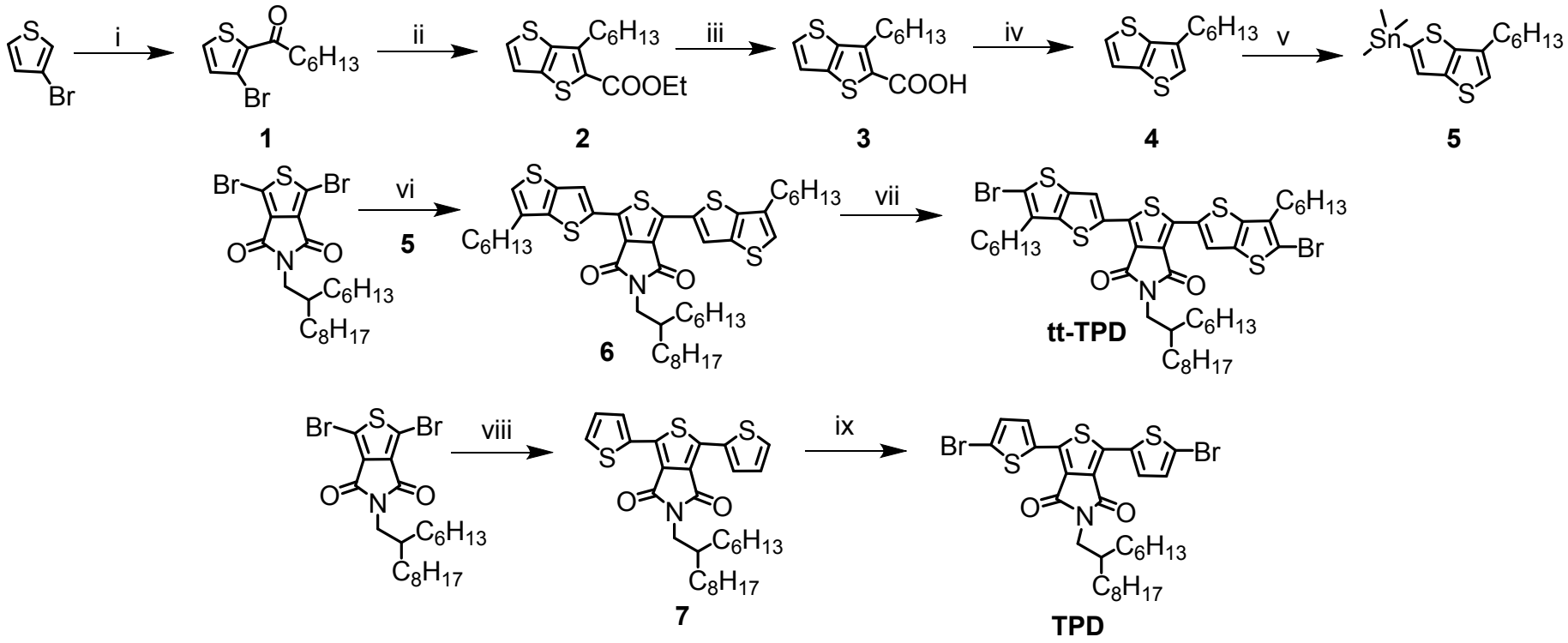

Scheme S1 Synthetic scheme for **tt-TPD** and **TPD** monomers : (i) $AlCl_3$, heptanoyl chloride, methylene chloride, 4 h, room temperature, Ar. (ii) K_2CO_3, ethyl mercaptoacetate, 18-crown-ether, 60 ^oC, 12h. (iii) NaOH, H_2O, THF, HCl, 80^oC, 12h. (iv) Cu, quinoline, 240 ^oC, 3h. (v) *n*-BuLi, trimethyltin chloride, -78^oC, 2h. (vi) Compound 5, $Pd(pph_3)_2Cl_2$, DMF, 150^oC, 12h. (vii) NBS, DMF, 8h. (viii) 2-Tributylstannylthiophene, $Pd(pph_3)_2Cl_2$, DMF, 150^oC, 12h. (ix) NBS, DMF, 8h.

Figure S1. TGA and DSC thermograms of the polymers.

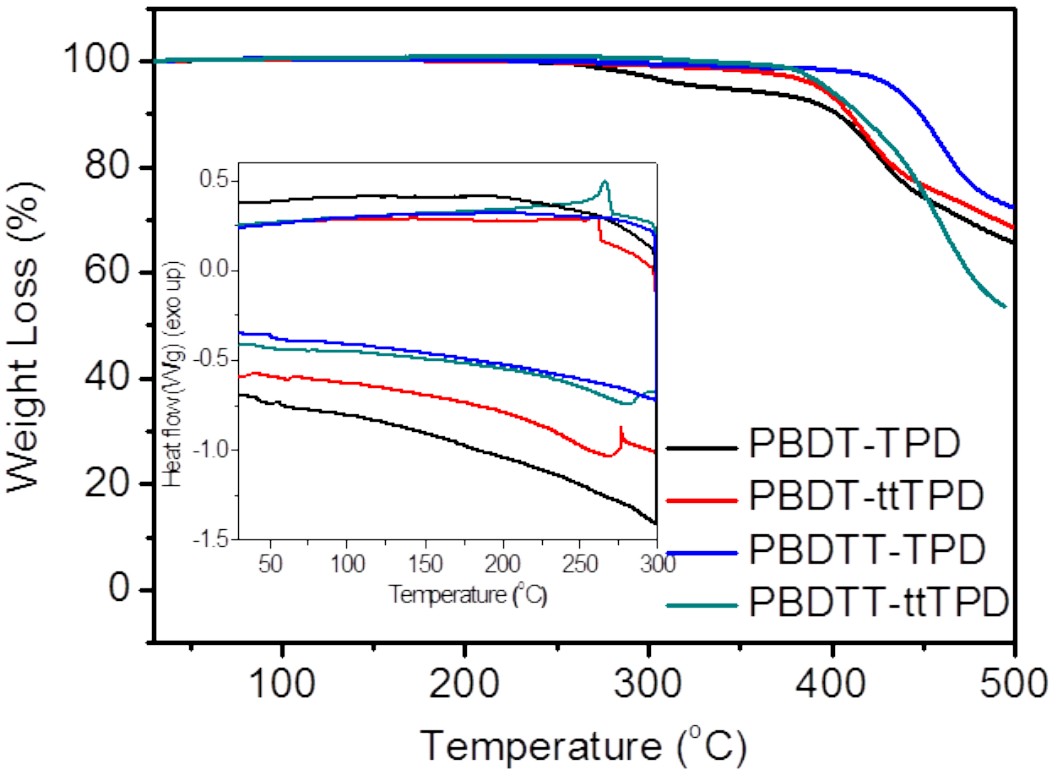

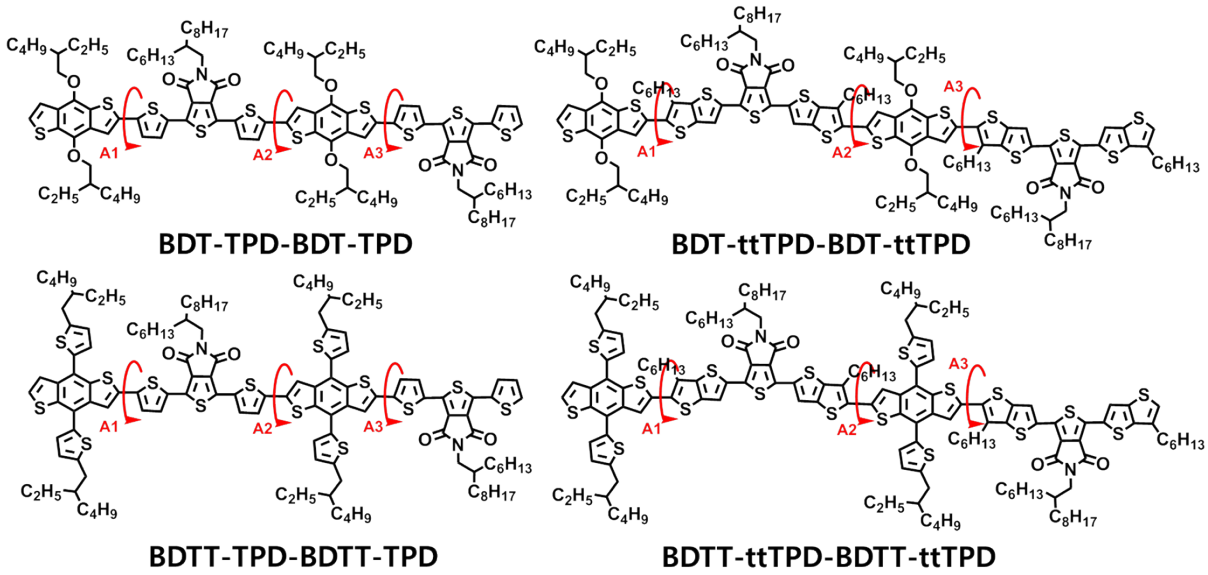

Polymer	Dihedral angle (°)		
	A1	A2	A3
PBDT-TPD	16.66	3.72	10.74
PBDT-ttTPD	40.99	47.19	45.39
PBDTT-TPD	21.73	13.31	1.89
PBDTT-ttTPD	35.76	43.20	43.07

Table S1. Dihedral angles of the model compounds calculated by density functional theory (DFT).

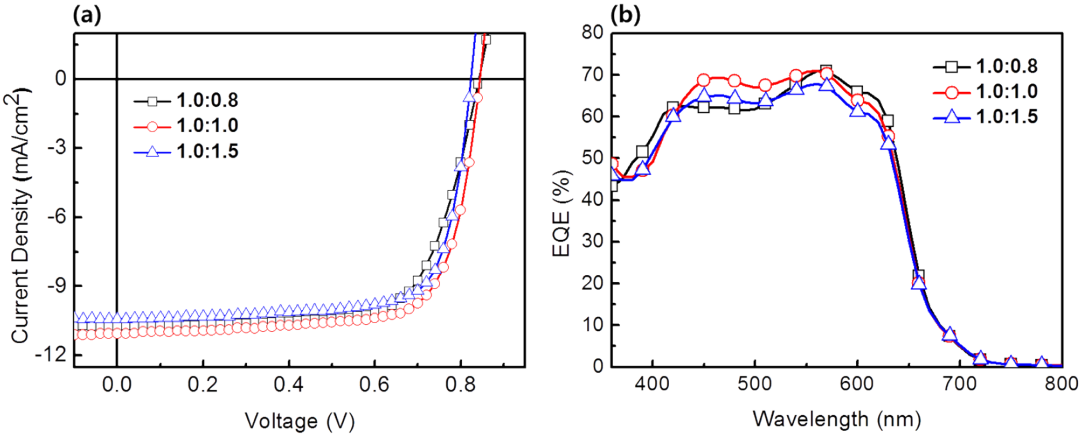

Figure S2. (a) *J*–*V* curves for ITO/ZnO NPs/PBDTT-ttTPD:$PC_{71}BM$ (processed with 3 vol% DIO)/MoO_3/Ag configuration with different weight ratios. (b) EQE curves of the OPVs based on PBDTT-ttTPD:$PC_{71}BM$ (processed with 3 vol% DIO) with different weight ratios.

Table S2. Comparison of the photovoltaic properties of the OPVs based on PBDTT-ttTPD:$PC_{71}BM$ (processed with 3 vol% DIO) with different weight ratios, measured under an illumination of AM 1.5 G, 100 mW cm^{-2}.

Polymer	Weight ratio [w/w]	V_{OC} [V]	J_{SC} [mA/cm^2]	*FF* [%]	PCE [%]
PBDTT-ttTPD: $PC_{71}BM$ with DIO	1.0:0.8	0.84	10.72	70	6.29
	1.0:1.0	0.84	11.05	73	6.81
	1.0:1.5	0.82	10.41	75	6.43

The device architecture is ITO/ZnO NPs/polymer:$PC_{71}BM$/MoO_3/Ag.

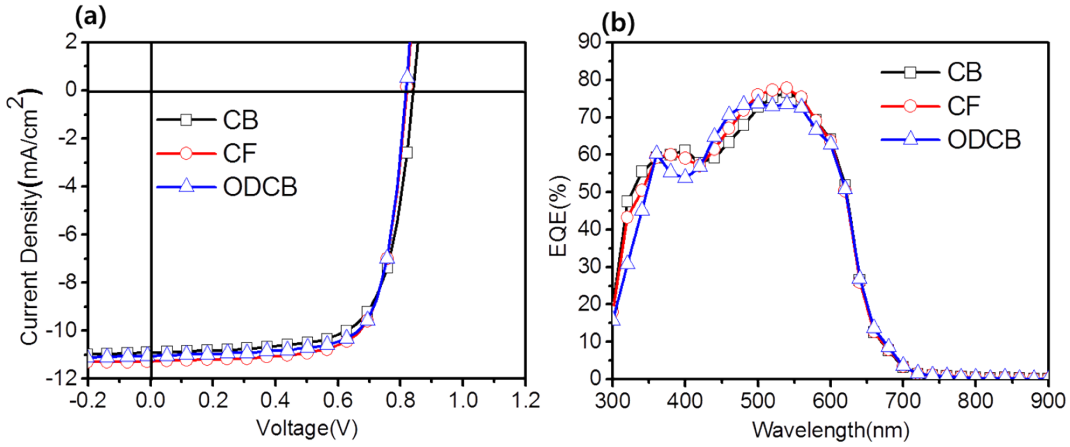

Figure S3. (a) *J–V* curves for ITO/ZnO NPs/PBDTT-ttTPD:$PC_{71}BM$ (1:1) (processed with 3 vol% DIO)/MoO_3/Ag configuration with different solvents. (b) EQE spectra of the OPVs based on PBDTT-ttTPD:$PC_{71}BM$ (1:1) with different solvents.

Table S3. Comparison of the photovoltaic properties of the OPVs based on PBDTT-ttTPD:$PC_{71}BM$ (1:1) with different solvents under an illumination of AM 1.5 G, 100 mW cm^{-2}.

Polymer	Solvent With DIO	Weight ratio [w/w]	V_{OC} [V]	J_{SC} [mA/cm^2]	*FF* [%]	PCE [%]
PBDTT-ttTPD : $PC_{71}BM$	CB	1.0:1.0	0.84	10.91	70	6.41
	CF	1.0:1.0	0.82	11.28	72	6.70
	ODCB	1.0:1.0	0.82	11.04	74	6.65

The device architecture is ITO/ZnO NPs/polymer:$PC_{71}BM$/MoO_3/Ag.

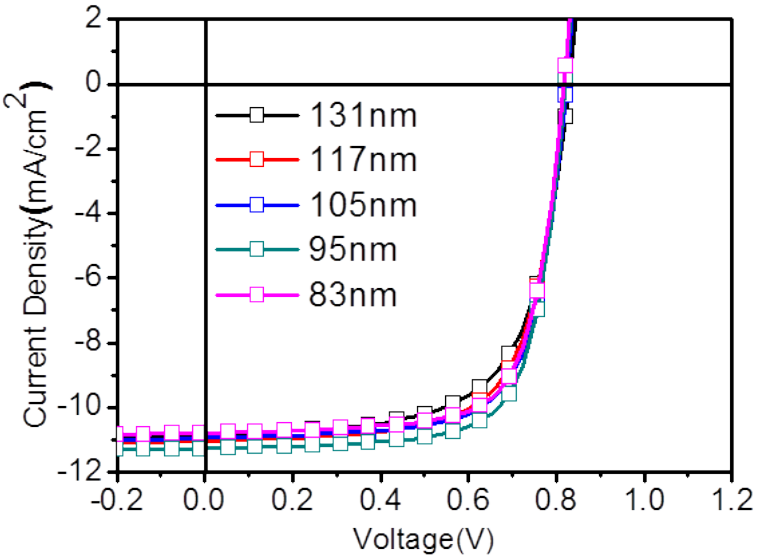

Figure S4. *J–V* curves for ITO/ZnO NPs/PBDTT-ttTPD:$PC_{71}BM$ (1:1) (CF solvent processed with 3 vol% DIO)/MoO_3/Ag configuration with different active layer thickness.

Table S4. Comparison of the photovoltaic properties of the OPVs based on PBDTT-ttTPD:$PC_{71}BM$ (1:1) with different active layer thicknesses under an illumination of AM 1.5 G, 100 mW cm^{-2}.

Polymer	Solvent	Thickness [nm]	V_{OC} [V]	J_{SC} [mA/cm^2]	*FF* [%]	*PCE* [%]
PBDTT-ttTPD : $PC_{71}BM$ [1:1, w/w]	CF+DIO	131	0.82	10.87	66	5.93
		117	0.82	11.05	69	6.22
		105	0.82	10.95	71	6.41
		95	0.84	11.05	73	6.81
		83	0.82	10.80	72	6.36

The device architecture is ITO/ZnO NPs/polymer:$PC_{71}BM$/MoO_3/Ag.

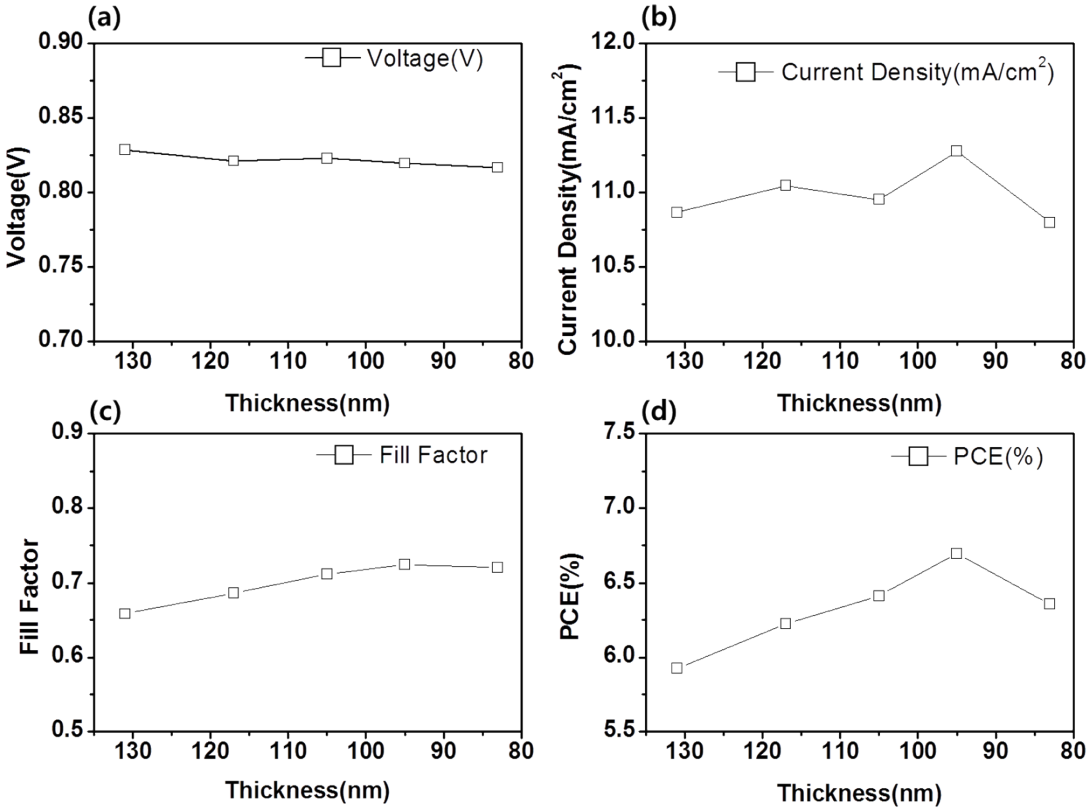

Figure S5. Photovoltaic parameters of the PBDTT-ttTPD:$PC_{71}BM$ OPVs under AM 1.5 G solar illumination: (a) Open-circuit voltage, (b) short-circuit current density, (c) fill factor, and (d) power conversion efficiency as a function of active layer thickness.

Table S5. Calculated hole mobilities of pure polymer and polymer:$PC_{71}BM$ system under optimized conditions as determined by SCLC.

Polymer	Thickness (nm)	μ_h[a] ($cm^2V^{-1}s^{-1}$)	Blend system (1:1, w/w)	Thickness (nm)	μ_h[a] ($cm^2V^{-1}s^{-1}$)
PBDT-TPD	90	1.34×10^{-5}	PBDT-TPD : $PC_{71}BM$	90	4.73×10^{-6}
PBDT-ttTPD	90	2.41×10^{-4}	PBDT-ttTPD : $PC_{71}BM$	90	2.53×10^{-5}
PBDTT-TPD	90	3.90×10^{-5}	PBDTT-TPD : $PC_{71}BM$	90	6.20×10^{-6}
PBDTT-ttTPD	90	7.20×10^{-4}	PBDTT-ttTPD : $PC_{71}BM$	90	3.08×10^{-5}

[a]Hole-only devices with ITO/PEDOT:PSS/pure polymer or polymer:$PC_{71}BM$ (1:1, w/w)/MoO_3/Au structure.

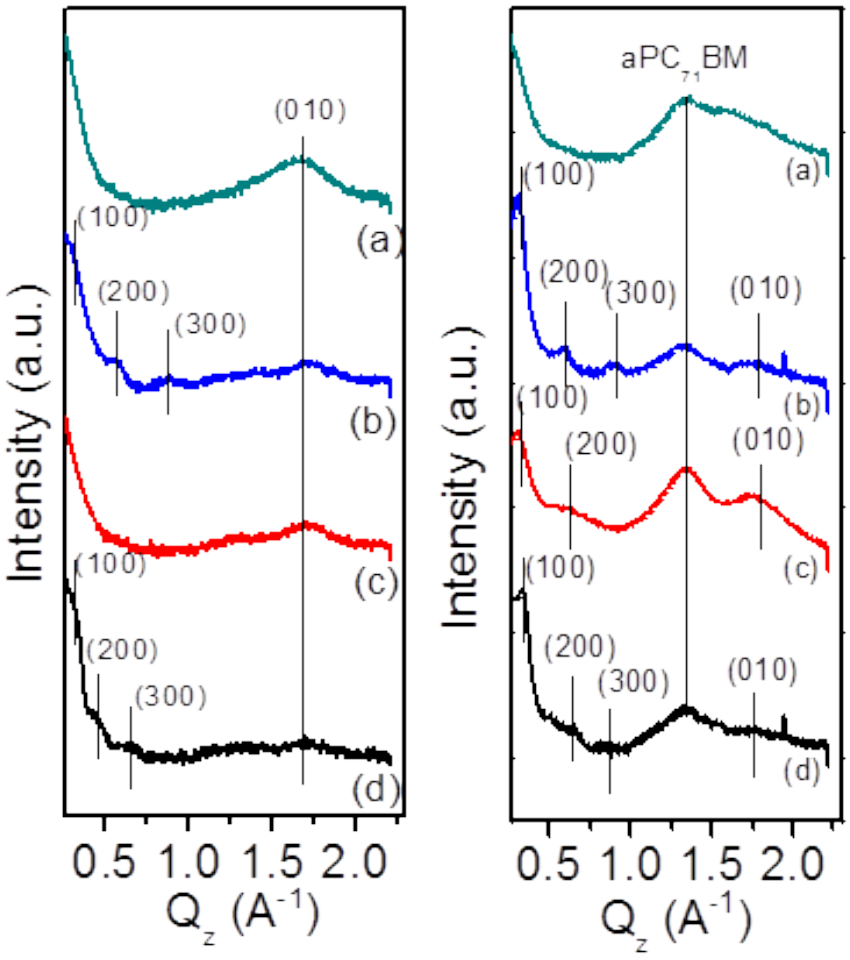

Figure S6. 1D out-of-plane X-ray profiles extracted from the 2D-GIXD patterns: (left) pure (a) PBDT-TPD, (b) PBDT-ttTPD, (c) PBDTT-TPD, and (d) PBDTT-ttTPD and (right) polymer:$PC_{71}BM$ (1:1 w/w) blend films: (a) PBDT-TPD, (b) PBDT-ttTPD, (c) PBDTT-TPD, and (d) PBDTT-ttTPD.

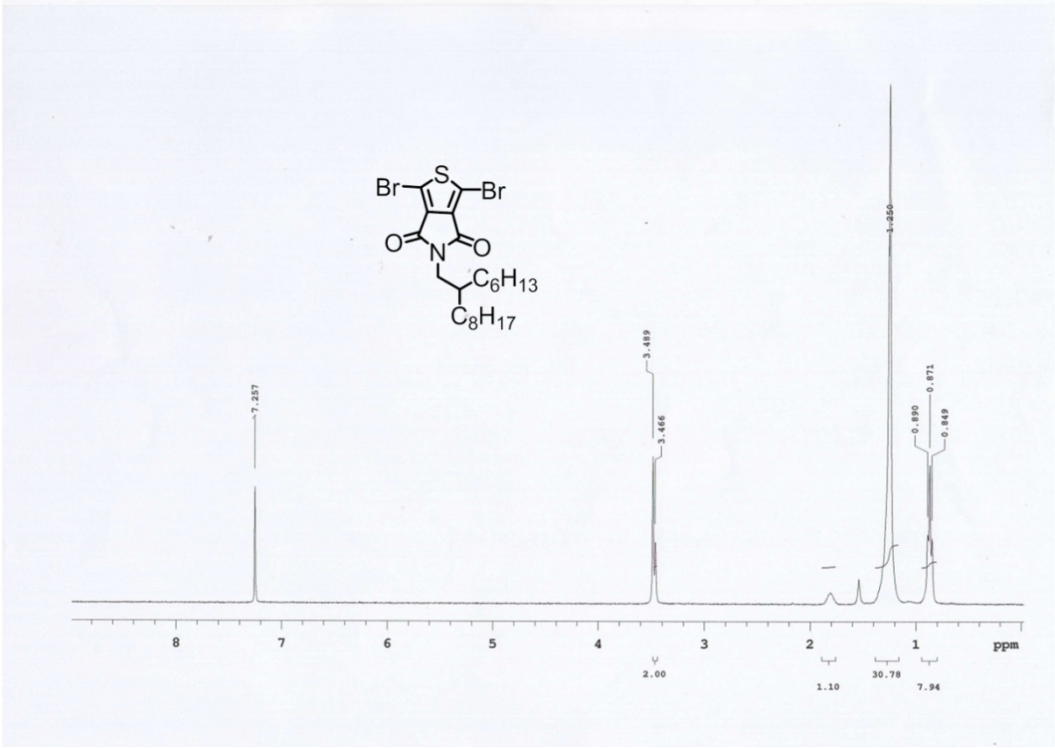

Figure S7. [1]H NMR spectrum of 1,3-dibromo-5-(2-hexyldecyl)-4H-thieno[3,4-c]pyrrole-4,6(5H)-dione.

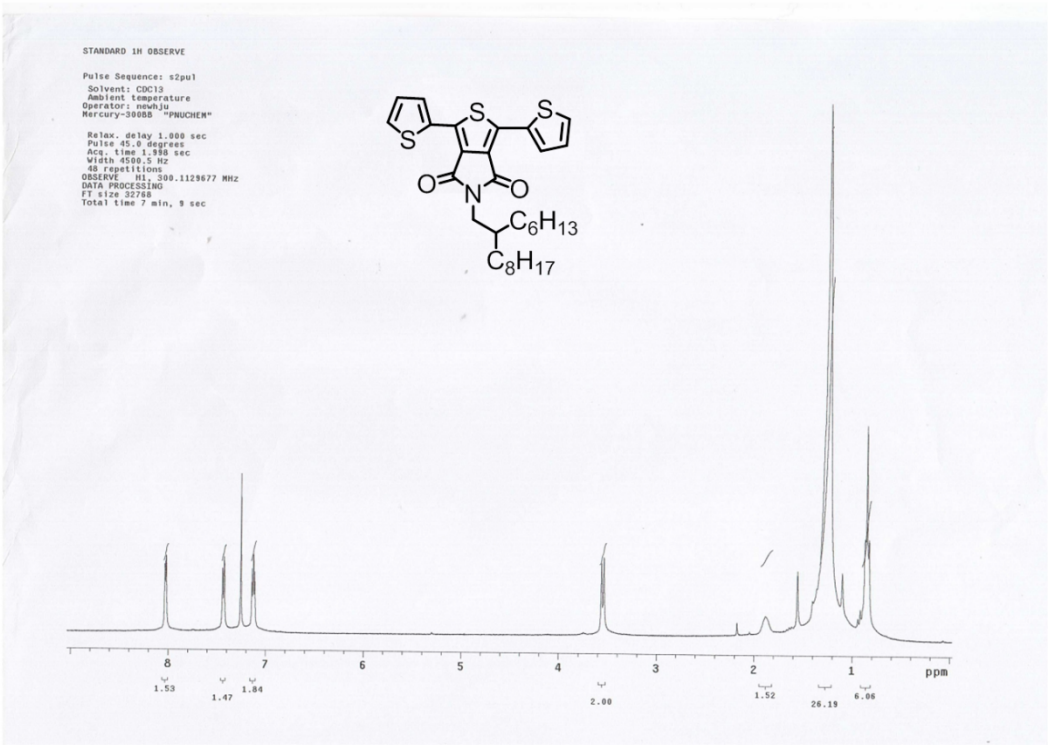

Figure S8. [1]H NMR spectrum of compound 7.

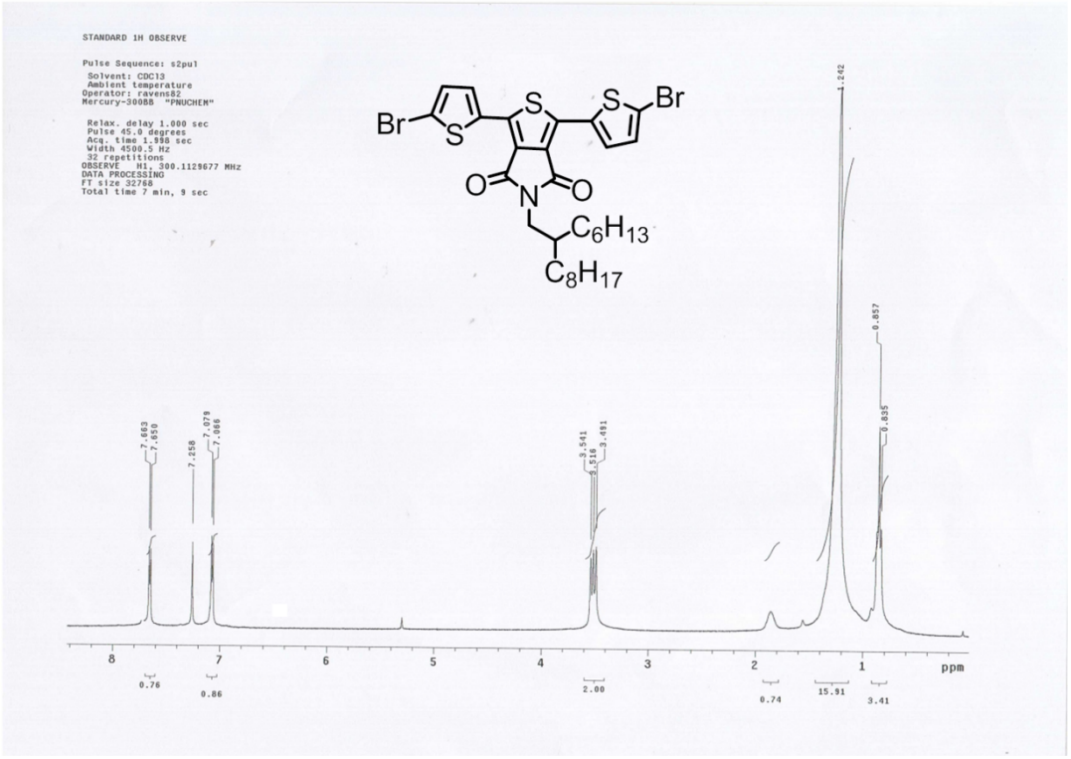

Figure S9. [1]H NMR spectrum of TPD.

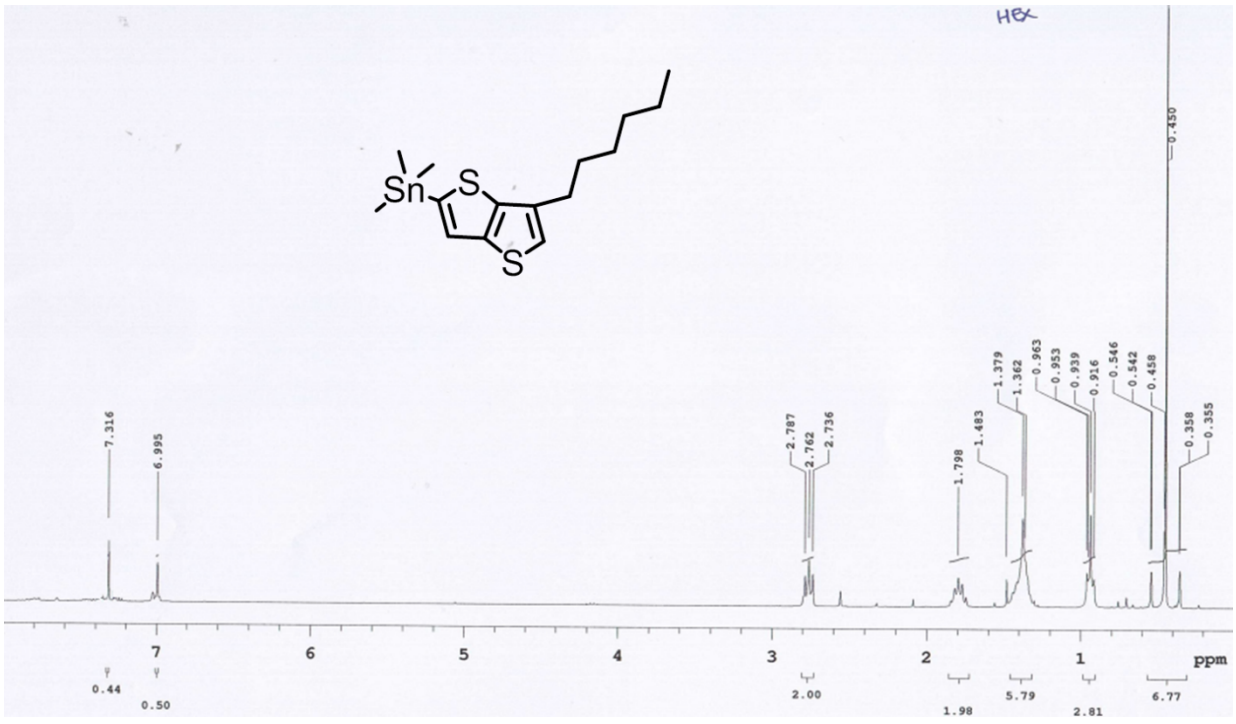

Figure S10. [1]H NMR spectrum of compound 5.

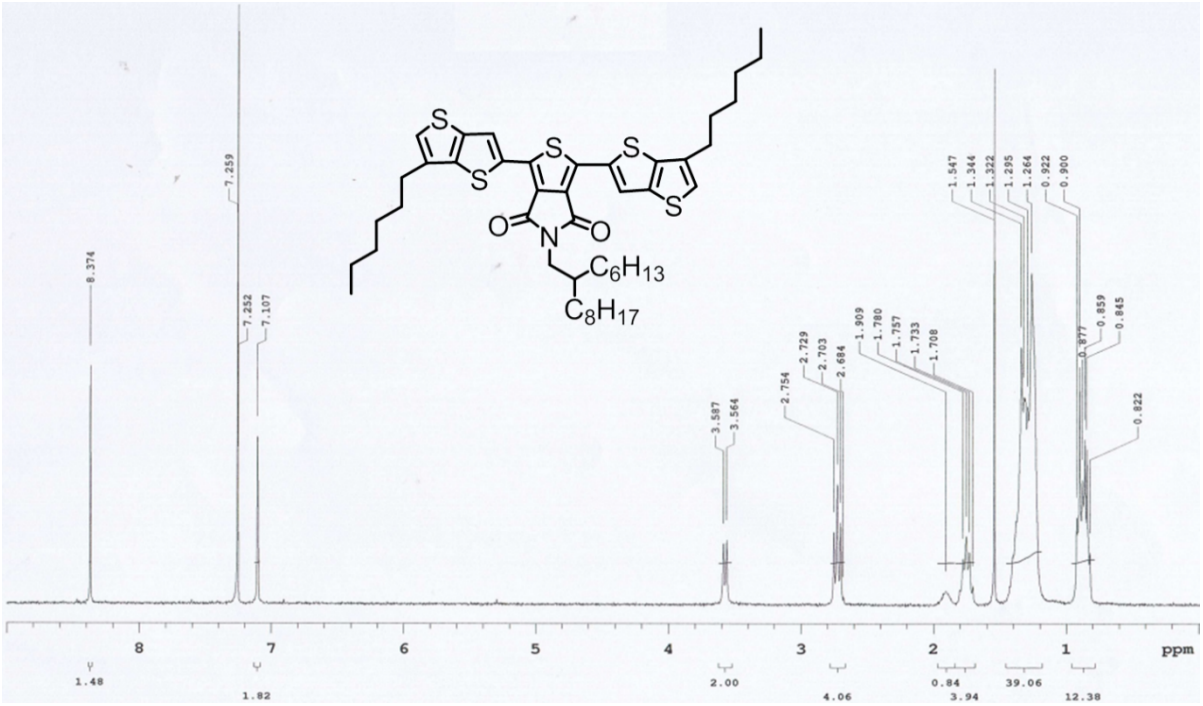

Figure S11. [1]H NMR spectrum of compound 6.

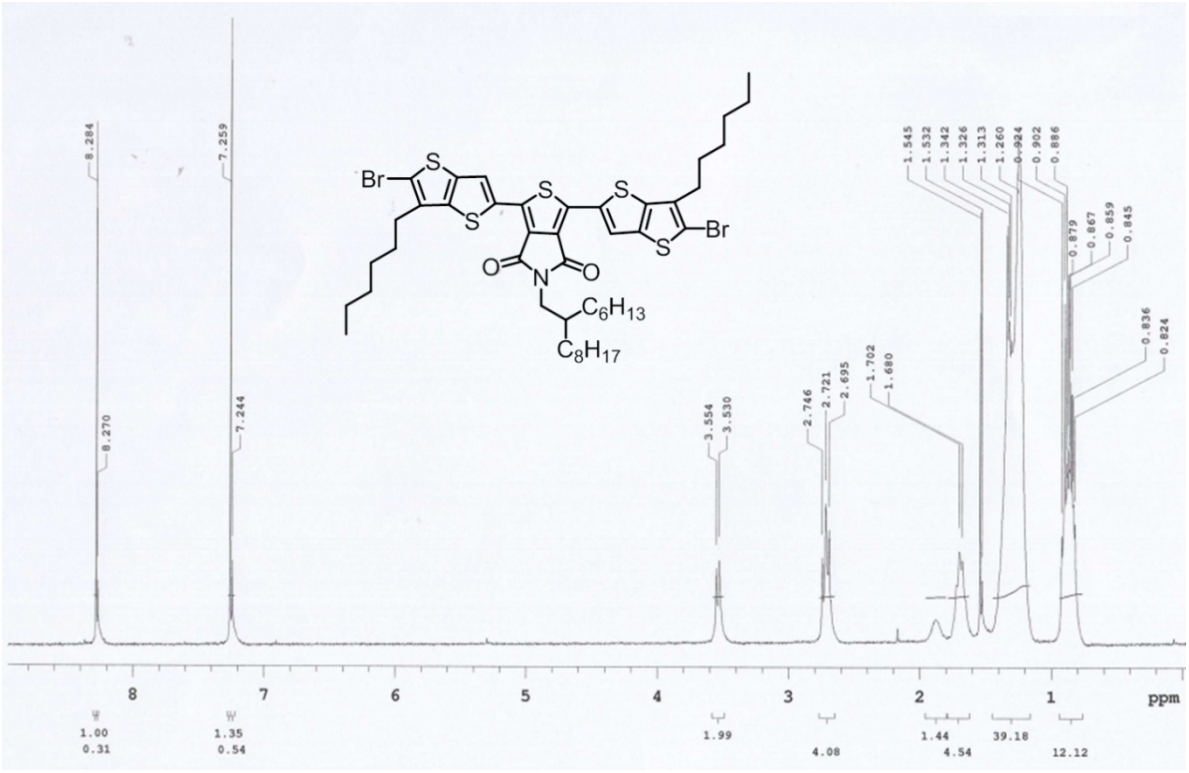

Figure S12. [1]H NMR spectrum of tt-TPD.